Proceedings of ASME Turbo Expo 2011
GT2011
June 6-10, 2011, Vancouver, British Columbia, Canada

GT2011-45610

AERO-THERMAL PERFORMANCE OF A COOLED WINGLET AT ENGINE REPRESENTATIVE MACH AND REYNOLDS NUMBERS

D. O. O'Dowd, Q. Zhang, L. He
Department of Engineering Science
University of Oxford
UK

B. C. Y. Cheong
Rolls-Royce plc
Turbine Systems (FH-3)
Bristol BS34 7QE
UK

I. Tibbott
Rolls-Royce plc
Turbine Systems
PO Box 31
Derby DE24 8BJ
UK

ABSTRACT

This paper presents an experimental investigation of the aero-thermal performance of a cooled winglet tip, under transonic conditions (exit Mach number of 1.0, and an exit Reynolds number of $1.27\text{x}10^6$, based on axial chord). Spatially-resolved heat transfer data and film cooling effectiveness data are obtained using the transient infrared thermography technique in the Oxford High-Speed Linear Cascade test facility. Aerodynamic loss data are obtained by traversing a specially-made and calibrated three-hole pressure probe and a single-hole probe one axial chord downstream of the blade. Detailed contours of Nusselt number show that for an increase in tip clearance, with and without film cooling, and for coolant injection, for both tip clearances, the Nusselt number increases. Also the smaller tip clearance observes higher film cooling effectiveness overall. Detailed distributions of kinetic energy losses as well as pitch-wise averaged loss coefficients and loss coefficients at a mixed-out plane indicate that the size of the loss core associated with the over-tip leakage vortex decreases with cooling injection.

1. INTRODUCTION

Over the past few decades, many engine manufacturers have been designing unshrouded high-pressure turbine blades in order to achieve increased rotation speeds and performance. Unshrouded blades rotate with a clearance relative to the liner segments. This tip clearance results in enhanced heat transfer on the tip as well as increased losses from the over-tip leakage (OTL) flow. To take advantage of the benefits from an unshrouded tip design, designers must find ways to minimize both the heat transfer and the losses.

First, a review of turbine blade heat transfer studies from fundamental examinations to full turbine rig testing and computational analysis was provided by Bunker [1]. In an effort to measure heat transfer under engine-realistic flow conditions, transonic rotor studies have been used to obtain tip heat transfer measurements, typically with thin film gauges. Such studies include Dunn et al., [2], Metzger et al. [3] and Thorpe et al. [4]. However, it is difficult to obtain detailed, spatially-resolved tip heat transfer results with rotor studies, whether under high-speed or low-speed conditions.

One of the first detailed, spatially-resolved heat transfer studies was performed experimentally by Bunker et al. [5] and computationally by Ameri et al. [6]. Other tip heat transfer experimental studies include Azad et al. [7], Kwak and Han [8] Teng et al. [9] and Newton et al. [10]. However, these studies were all performed with exit $M_{exit} < 0.75$, with the latter two at low-speed, incompressible conditions.

To reduce OTL flow, different tip designs, such as squealers and winglets, are frequently examined. Heat transfer studies that have considered squealers include [11-15]. Mischo et al. [16] examined squealer tips in a one and a half stage turbine. Experiments show that the squealer helps reduce both suction side and tip heat transfer. Dunn and Haldeman [17] measured heat transfer using thin-film heat flux gauges on a recessed tip on a transonic turbine blade in a full-stage rotating turbine. Others have also investigated squealers with tip film cooling include [18-23].

As an alternative to the squealer, few experimental heat transfer studies have been performed on winglet tips, such as Papa et al. [24]. Saha et al. [25] computationally investigated heat transfer for different forms of a winglet on flat tips and squealer tips. They conclude that the double-sided squealer with winglet produces only marginal improvements in heat transfer coefficient. Though the study by Saha et al. is under transonic conditions, the maximum tip Mach number doesn't quite reach sonic conditions. O'Dowd et al. [26] examined heat transfer on a blade with a winglet tip under transonic conditions. However, to the best of the author's knowledge, there are no spatially-resolved experimental heat transfer studies on a cooled winglet under transonic conditions.

The second part of the present study considers aerodynamic loss, specifically losses measured downstream of a blade row. Aerodynamic loss has been thoroughly addressed by Denton [27]. Very few rotor studies examine aerodynamic loss as it is challenging to measure loss downstream of a rotor. Rotor studies that experimentally consider aerodynamic loss are done so under subsonic conditions such as Xiao et al. [28], McCarter et al. [29] and Rao et al. [30].

Most of the highly-resolved aerodynamic loss studies are done using cascades, many of which are annular cascades testing nozzle guide vanes, which do not examine OTL losses. Some of these studies have used the same definition of aero loss coefficient that is used in the present study, like Main et al. [31]. Unshrouded turbine blades are frequently examined in linear cascades. One of the first experimental aerodynamic loss studies was by Bindon [32] in a low-speed linear cascade, who not only measured the tip clearance loss, but determined relative proportions of the total tip clearance endwall loss to three basic components: internal gap loss, mixing loss of the OTL vortex with the passage flow, and secondary and endwall losses. Other experimental loss studies include Yamamoto [33] and Palafox et al. [34], who examined aerodynamic loss over flat tips under low-speed conditions.

In order to minimize OTL loss, different tip configurations are used. Heyes et al. [35] considered squealers under low-speed conditions. Like the heat transfer studies, few experimental aerodynamic loss studies have been done under high-speed, operationally representative conditions. Key and Arts [36] examined the aerodynamic loss of a squealer under transonic conditions while Hofer and Arts [37] examined a cooled squealer, using a similar definition of loss as in the present study (Eq. (5)), though Hofer and Arts used the local static pressure in the denominator, whereas the present study uses a mid-span averaged value for all points in the contour.

Few have investigated the winglet. Early studies include Wadia and Booth [38] and Yaras et al. [39]. Dey and Camci [40] examined a flat tip blade with pitch-wise extensions much like a winglet, using a low-speed rotor. Schabowski and Hodson [41] considered both squealer and winglet aerodynamic loss and Schabowski et al. [42] optimized a combined winglet-squealer design. All of these winglet studies, however, have been under low-speed, if not subsonic conditions.

Saha et al. [25] numerically predicted the aerodynamic loss of a winglet tip under transonic conditions, but with an unchoked tip. Based on initial computational work by Harvey and Ramsden [43], Harvey et al. [44] and Willer et al. [45] measured exit flow conditions for their winglet design in a high-speed rotor. However, to the best of the author's knowledge, there have been no published experimental aerodynamic loss studies for cooled winglets under experimentally-representative transonic conditions.

As mentioned above, few aero-thermal examinations have been performed under engine-realistic aerodynamic conditions. Though there appears to be some consensus on heat transfer and aerodynamic loss for both plain tips and squealer tips under low-speed conditions, there are little understanding whether these low-speed studies can be scaled up to engine-operating conditions. Moore et al. [46] demonstrated using a water table and the hydraulic analogy that there is a shock structure over the tip which is related to enhanced heat transfer on the tip. This study was experimentally confirmed by Zhang et al. [47]. Wheeler et al [48] computationally compared heat transfer and OTL flow for different exit Mach number conditions. First, to ensure that the blade loading was the same for all tests, the geometry was altered. Second, results showed that for transonic flow conditions, shocks occur over the tip. If parts of the tip are choked [26,49], and if a shock structure exists over certain parts of the blade, it is unreasonable to assume the heat transfer and the loss stays the same as under low-speed conditions. The present authors argue that the low-speed results cannot simply be extrapolated to high-speed conditions. With the addition of tip film cooling, the aero-thermal impact on an engine-representative blade is even less understood.

Finally, conventional wisdom suggests that coolant injection almost always enhances aerodynamic loss. It is currently not known if this is always the case. Using a water table, Wadia and Booth [38] showed that coolant injection reduced the OTL flow. Krishnababu et al. [23] observed that coolant flow partially blocked the tip gap, reducing the area available for the OTL flow. Hofer and Arts [37], determining a global mass-weighted thermodynamic loss coefficient in a high-speed linear cascade, showed that coolant injection had a marginal effect on the loss coefficient, where in some cases, loss is slightly reduced.

The present investigation focuses on tip heat transfer as well as the aerodynamic loss downstream of the blade row for a modern winglet with and without coolant injection for two different tip gaps (1.0% and 1.5% of the engine-equivalent span) under engine-representative aerodynamic flow conditions in a linear cascade. Spatially-resolved Nusselt numbers and film cooling effectiveness on the blade tip are experimentally determined using the transient infrared thermography technique. Spatially-resolved exit flow conditions are measured using a three-hole and single-hole probe one axial chord-distance downstream of the blade row. The relationship between heat transfer and aerodynamics are closely coupled and it is important to examine the effect of transonic flow conditions on both heat transfer and aerodynamic loss.

The overall objectives for this experimental study are to both enhance the understanding of complex aero-thermal performance in the tip region at engine representative aerodynamic conditions and to validate future CFD modeling and predictive capabilities for such a challenging problem of practical interest.

Note that all figures showing blade geometry have been intentionally distorted for reasons of company confidentiality.

2. EXPERIMENTAL SETUP

The experiments are conducted at the University of Oxford's High Speed Linear Cascade (HSLC). Figure 1 shows the schematic of the HSLC.

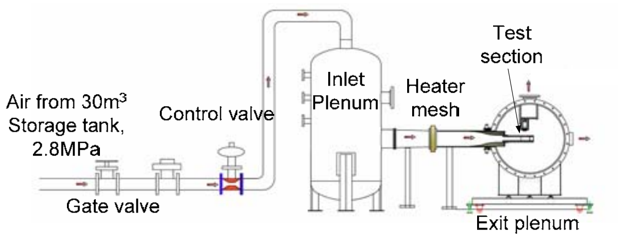

Fig. 1 The schematic of the Oxford high speed linear cascade research facility

2.8MPa (400psi) compressed air is stored in a 30 m^3 storage tank. A 203 mm (8 in.) gate valve, a 203mm (8 in.) Worcester Ball valve with an air operated actuator, and a Spirax-Sarco control valve/actuator/positioner is located downstream of the air storage tank. A Spirax-Sarco X5 PID process controller regulates the pressure in the test section as the storage tank discharges. An inlet plenum tank is located downstream of the control valve. A heater mesh element is installed between transition ducts to provide a step increase in mainstream flow temperature. The heater mesh is described in Gillespie et al. [50]. During each blow down test, 100 kW electrical power is dissipated in the heater mesh to raise the mainstream temperature by 25°C, when operating at 100V.

The test section is mounted inside the exit plenum, as shown in Fig. 1. Other components in the exit plenum include an infrared camera, traversing system, a closed-circuit television camera and lighting. Figure 2 shows the details of the test section with 4 passages and 5 blades (including two sidewalls representing a suction side and a pressure side). Boundary layer bleeds are built on all four inlet duct walls, which ensure an appropriate cascade flow condition. One movable tailboard is attached to the suction side sidewall. During the commissioning of the test rig, the boundary layer bleeds and tailboard are adjusted to achieve near periodic flow condition. Note that the pressure side tailboard was removed following observations related to the flow periodicity and concerns about shock wave reflections.

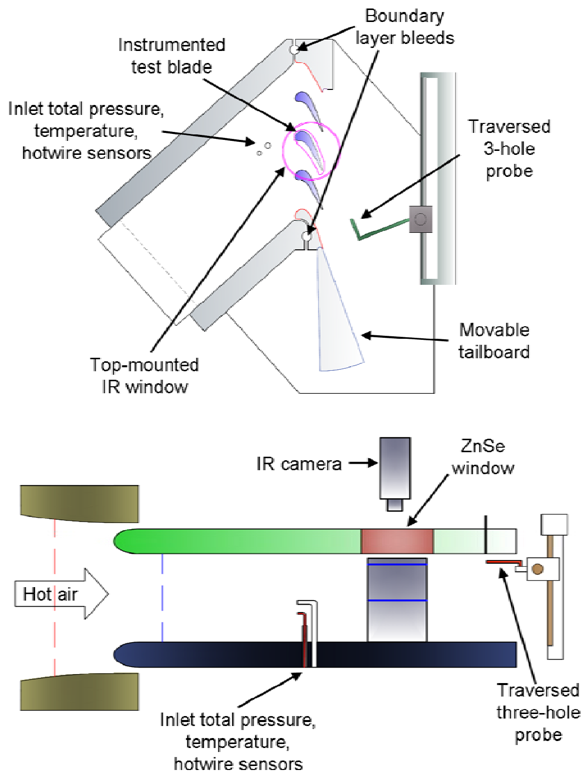

Fig. 2 The schematics of the test section and instrumentation

A Zinc-Selenide (ZnSe) window is placed on the top casing wall so that the central test blade tip surface is accessible to an infrared camera (FLIR A325) for spatially-resolved surface temperature measurements, as shown in Fig. 2. A three-hole probe is traversed one axial-chord downstream of the blade row, also shown in Fig. 2.

Figure 3 shows both the uncooled and the cooled winglet-tip geometries employed in the present study, which are scaled larger than the actual turbine blade [51]. The uncooled winglet geometry is very similar to the design presented by [44,45], with the exception of the pressure side recess. The design motivation for the uncooled winglet is based on work by Harvey and Ramsden [43] who proposed an alternate means of controlling the OTL loss by modifying the local surface velocities at the rotor tip, particularly by increasing the velocity at the pressure-side overhang. According to Harvey and Ramsden, the pressure-side overhang is intended to increase blockage and thus lower the local static pressure driving the OTL flow. In addition, the gutter allows for chordwise leakage flow from the leading edge. The follow-up work by Refs. [44-45] further modified the winglet, but did not consider cavities (or recesses), and recommended further optimization to include cavities in order to reduce loss and heat transfer. Also, cavities decrease the amount of material that can contact the casing wall and will also lessen the weight of the blade.

The tip surface is made of epoxy with very low thermal conductivity and is also instrumented with thermocouples (mainly for the purpose of an *in-situ* IR calibration). The uncooled winglet has no cooling holes whereas the cooled winglet has cooling holes on the pressure-side lip overhang and on the suction side inward surface of the gutter. The tip clearance for the three center blades is adjustable.

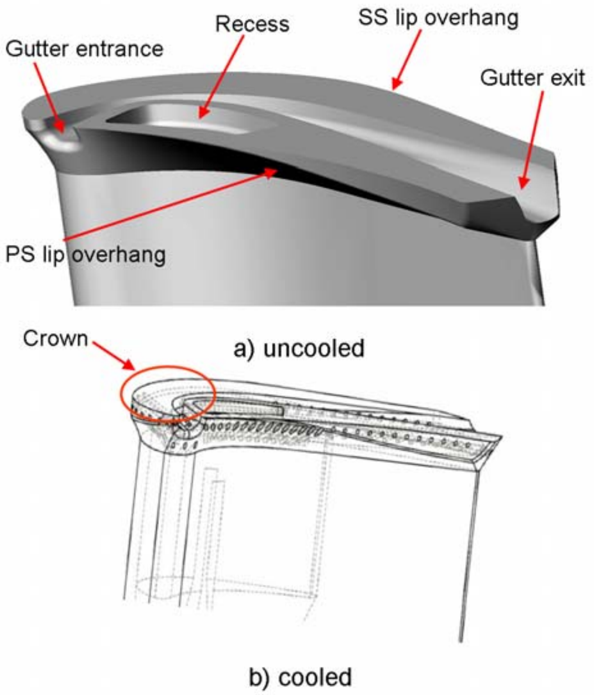

Fig. 3 The schematics of the winglet tips tested in the HSLC (slightly modified from [44,45]) for the (a) uncooled winglet and (b) cooled winglet

The PID feedback control system enables a steady flow at the inlet of the test section during every blow-down test. A relatively constant total pressure of 200kpa (absolute) can be maintained for about 90 seconds. LabVIEW 8.6 is employed for data acquisition programming.

Table 1 Transonic flow conditions of the test rig (same as tested in [51].

Inlet total pressure	200 kPa
Inlet Mach number	0.28
Inlet Reynolds number (based on axial chord)	0.60×10^6
Mass flow rate	3.23 kg/sec
Exit Mach number	1.0
Exit Reynolds Number (based on axial chord)	1.27×10^6

At the inlet to the test section, a pitot-static probe and a total temperature thermocouple are located one axial-chord upstream of the blades. A total pressure rake is also used to determine the inlet flow uniformity throughout the inlet. A hotwire survey is conducted one axial-chord upstream of the test blade to measure the inlet turbulence and inlet casing wall boundary layer profile. The inlet casing wall turbulent boundary layer thickness is about 4mm (approximately 8% of C_x). Measured flow conditions are included in Tab. 1. The pressure loading is measured to show an aft-loaded blade with a Mach number distribution typical for high-pressure turbine blades. Further details of the experimental setup are described in O'Dowd et al. [51].

3. COOLANT SETUP

The HSLC is modified to provide coolant to the cooled winglet. As observed in O'Dowd et al. [26], low adiabatic wall temperatures were calculated on the trailing edge region of the tip due to high flow speeds. Therefore, the coolant temperature must be lower than the lowest adiabatic wall temperature determined on the blade tip.

100psi pressure (689 kPa) of room-temperature air is supplied to 3 linked vortex tubes, which can be adjusted to provide a 0—40°C temperature drop, depending on the output pressure required. Compressed air enters the vortex tubes, at which point the high-energy air moves to the outside of the vortex generator radius while the low-energy air moves to the inside of the vortex generator radius and exits the vortex tube toward the HSLC. To prevent the coolant from absorbing ambient thermal energy, the coolant pipes are insulated. The coolant then enters a settling chamber inside the test plenum, as shown in Fig. 4. The coolant must vent for at least 30 minutes to ensure that the coolant feed and piping temperatures are stable. However, this would pre-cool the winglet and affect heat transfer measurements. A solenoid switch is added to bypass the coolant air until the temperature is stable (measured in the settling chamber) and is directed to the blade during a test run.

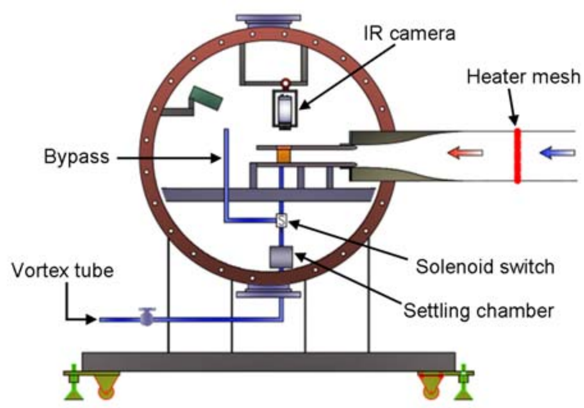

Fig. 4 Schematic of test plenum, including coolant supply, settling chamber, solenoid switch and bypass feed

The current study only considers tip film cooling injection. During testing, pressure and temperature measurements are obtained in a reservoir inside the test blade. The total pressure ratio between the coolant and mainstream flows is approximately 1.08. The temperature ratio between the mainstream and coolant flows for the heat transfer study is approximately 1.1.

Prior to using the vortex tubes, a sonic orifice plate is used to determine the coolant mass flow rate for a tip clearance of 1.5% of engine-equivalent span, which is approximately 1.19% of the HSLC mainstream mass flow rate, or 0.80% of the engine-equivalent mass flow rate, based on blade span and pitch. When changing tip clearances, the coolant to mainstream pressure ratio is kept constant. The static pressure distribution near the cooling holes is expected to vary with changes in tip clearance. However, for a constant coolant pressure ratio, the variation in mass flow rate is expected to be minor. Also, impact of this variation on the heat transfer and aerodynamic loss is expected to be minimal.

An examination of the test section periodicity showed the requirement to use the same blade geometry for all three blades during a single test. The three center blades all have winglet tips. In addition, for aerodynamic loss measurements, all three center blades inject coolant in order to obtain periodicity. For heat transfer, on the other hand, obtaining a temperature ratio that allowed for a sensible value of film cooling effectiveness meant that only the center blade could inject coolant with the limited pressure supply. Though downstream periodicity is not obtained for the heat transfer examination of the cooled winglet, the tip heat transfer is not expected to significantly change with the absence of cooling injection from the adjacent blades.

4. AERO-THERMAL MEASUREMENT TECHNIQUES

Heat transfer measurement technique

A transient thermal measurement technique is employed in the current study. As previously indicated, an abrupt step-change in the mainstream temperature is achieved by the heater mesh installed upstream of the test section. During each blow-down test, the spatially-resolved temperature history for the tip surface is recorded by an IR camera. The heat transfer to the blade tip surface is considered to be to a semi-infinite solid domain since the tip material has low conductivity and the thermal penetration depth is small during a tunnel run. A complete heat flux history is then reconstructed from temperature traces for each blade tip location using the Impulse method described by Oldfield for use with thin film gauges [52] and implemented using an IR camera by [51]. This method uses known pairs of exact solutions to derive an impulse response digital filter to convert temperature into heat flux using Fast Fourier Transforms.

The reconstruction of the heat flux from the temperature trace leads to a plot of the heat flux variation versus the wall temperature. Due to minor variations in the mainstream pressure caused by regulated valve movement, the heat flux and temperature are non-dimensionalized. A linear relationship between the heat flux and wall temperature is expected and also observed. Here, the heat transfer coefficient for the blade tip is defined using

$$\dot{q} = h(T_{ad} - T_w) \qquad (1)$$

Therefore, the slope of the non-dimensionalized heat flux versus wall temperature is proportional to the local heat transfer coefficient, and the adiabatic wall temperature can be extrapolated for zero heat flux. This reconstruction method is then used for all the tip surface locations (320x240 IR pixel resolution).

The surface Nusselt numbers are then determined from the heat transfer coefficient, h. The conductivity of air, k_{air}, is calculated based on the local adiabatic wall temperature and C_x is the axial chord of the blade.

$$Nu = \frac{hC_x}{k_{air}} \qquad (2)$$

The experimental uncertainties are determined using a combination of partial derivatives described by Kline and McClintock [53], a jitter analysis described by Moffat [54] and the standard error of estimate resulting from the errors created when determining the IR calibration curve, as described in Coleman and Steele [55]. The overall uncertainty for Nusselt number is 9.5%, and uncertainty for adiabatic wall temperature is 1.2K (4.8% of the rise in mainstream temperature during the transient). Reproducibility of heat transfer results is determined from multiple test runs. The area-weighted average of the normalized standard deviation is less than 6%. A detailed uncertainty analysis and qualification of the current heat transfer measurement technique is presented by O’Dowd [51].

Note that the 1-D conduction assumption used in the present study is unlikely to be accurate close to the corner edges and cooling holes. Thus higher uncertainties exist when the edges are approached.

Aerodynamic loss measurement technique

A two-dimensional downstream traverse system driven by a stepper-motor is employed to obtain total pressure surveys. A three-hole probe is employed in the present study to obtain detailed downstream pressure measurements. To resolve the near casing endwall region pressure field, a smaller, single-hole probe is used. The single-hole probe is also mechanically rotated at 3 different angles to obtain the maximum total pressure and approximate flow angle.

Measurements are taken one axial chord downstream of the central blade trailing edge. Pressure measurements are taken at eleven span-wise locations (from 75% to 100% of the engine-equivalent blade span), and twenty-four pitch-wise locations. After each step-wise traverse, data collection is delayed for one second in order to ensure the flow around the probe, sting and stem is stable. One-second of data is then recorded at each step-wise location to ensure enough response time for the transducer to obtain the appropriate reading.

The three-hole probe is calibrated in a transonic tunnel at the University of Oxford. Yaw, total pressure and Mach coefficients are calculated during the calibration and an analysis of the results yields an application matrix. Flow angle, total pressure and Mach number are obtained by linear interpolation and lookup of the application matrix. The computation technique is described by Main et al. [31].

The experimental uncertainties are determined using the method of Kline and McClintock [53]. By substituting the calibration data back into the application matrix and computing P_t, β and M at each point, the uncertainty magnitudes of probe measurements are determined. The uncertainties of P_t, M, and P_s are based on the RMS differences between the data over the whole field. The uncertainty in measured exit total pressure is less than 1%.

In the present study, a three-hole probe is used. This leads to additional uncertainty by not accounting for the pitch (span-wise) flow direction, but this angle is not expected to be greater than the yaw angle deviation from the metal exit angle. Within the OTL vortex, the center-hole channel measurement at 20° yaw angle differs from the true total pressure by 2.8%. This gives an indication of the maximum error (overestimate). More details about the probe design, the calibration and the uncertainty analysis are provided by O'Dowd et al. [56].

Computation details

O'Dowd et al. [26] conducted a combined experimental and computational study on the uncooled winglet. CFD predictions employed the Rolls-Royce HYDRA suite under the same flow conditions as those in the HSLC experiments. Steady RANS calculations were performed and the Spalart-Allmaras turbulence model was adopted. The computational domain consisted of one blade passage with periodic boundary conditions. The blade definition, tip gap clearance, flow angle, and inlet boundary conditions were kept exactly the same as the experimental setup.

Multi-block hexahedra mesh was generated by using ICEM. No "wall function" was employed in the study. The total grid size was about 9.9 million cells. For most of the winglet tip surface, y^+ values were around 1. Grid sensitivity studies were conducted to ensure that the mesh employed was grid independent in terms of heat flux.

The same computation model used for [26] is used in the present investigation. The present study employs the CFD analysis to calculate the local Mach number on the tip, halfway between the tip and the tip casing endwall for both tip gaps.

5. TIP HEAT TRANSFER RESULTS

A winglet is tested at two tip clearances both with and without tip film cooling. Figure 5 presents the contours of the experimentally-determined Nusselt number (Nu) for the blade tip with a tip gap clearance of 1.5%. Note that the Nusselt number contour for the uncooled winglet was presented in [26], which agreed well qualitatively with the predicted Nusselt number. In general, Fig. 5 shows a large increase in Nusselt number with cooling injection.

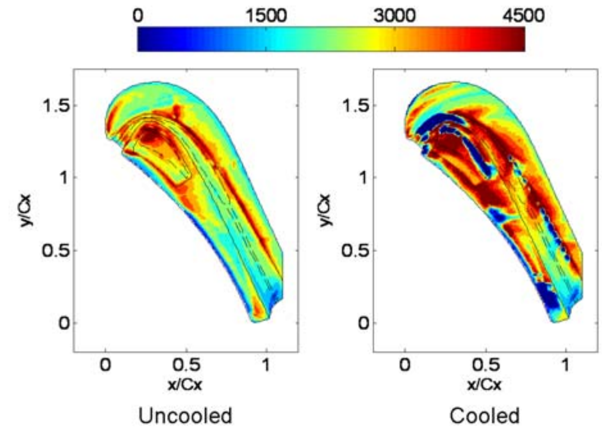

Fig. 5 Experimental Nusselt number for 1.5% tip clearance for the uncooled and cooled winglets

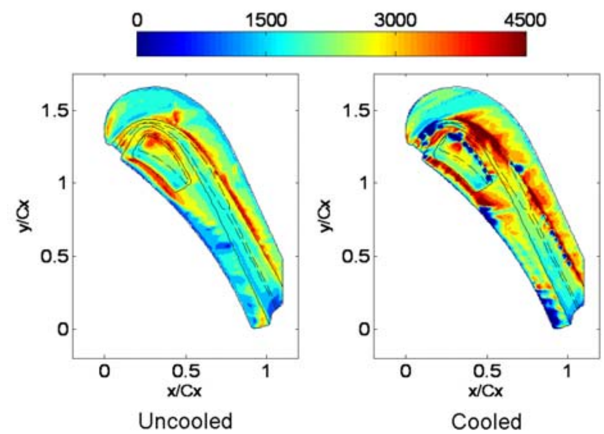

Fig. 6 Experimental Nusselt number for 1.0% tip clearance for the uncooled and cooled winglets

Decreases in Nusselt number are noted in regions where coolant holes are located, though there is an increase in Nusselt number in regions of close proximity to the films. Like the uncooled winglet, the cooled winglet shows a region on the pressure side edge from approximately 55—80% C_x of repeated striping of high and low Nusselt numbers that has been previously observed by [26,47,49,51].

As the tip gap is decreased to 1.0%, contours of the tip Nusselt number generally decrease, as shown in Fig. 6. The reduction in tip clearance leads to a reduction in mass flow through the tip and therefore less heat transfer. This is true for both the uncooled and cooled winglets. The general increase in Nusselt number between the uncooled and cooled winglet for the 1.0% tip gap is consistent with the 1.5% tip gap results.

Circumferentially-averaged Nusselt numbers for both tip clearances and for both uncooled and cooled cases is presented in Fig. 7. For both the uncooled and cooled winglets, an increase in tip clearance results in enhanced heat transfer except near the trailing edge for 90—100% axial chord (80-100% C_x for the cooled winglet), which is explained below with the help of the Mach number contours. For both the 1.0% and 1.5% tip clearances, coolant injection generally shows heat transfer enhancement, except toward the leading edge (first 15% C_x) and near the trailing edge (80—90% C_x). The 80—90% C_x region is the location on the pressure-side trailing edge corner where the uncooled winglet has high heat transfer and the cooled winglet has very low heat transfer.

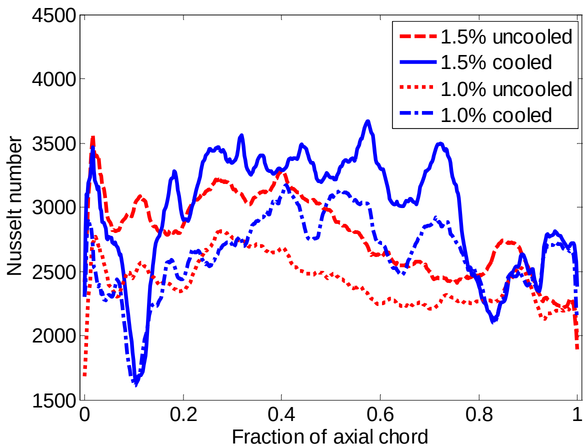

Fig. 7 Experimental circumferentially-averaged Nusselt number both uncooled and cooled winglet for 1.0% and 1.5% tip clearances

Experimental contours of local film cooling effectiveness are also obtained. Equation (3) shows the definition of film cooling effectiveness used in the present study,

$$\eta = \frac{T_{rec} - T_{ad}}{T_{rec} - T_c} \tag{3}$$

where T_{rec} is the local recovery temperature at each tip location, determined with no coolant injection using the uncooled blade, T_{ad} is the local adiabatic wall temperature at each tip location of the cooled winglet, and T_c is the coolant temperature, which is less than the lowest adiabatic wall temperature. For high speed flow conditions, using the mainstream temperature as the driving temperature is insufficient as the local recovery temperature is significantly different for transonic flow conditions. Figure 8 shows the film cooling effectiveness for both the 1.5% and 1.0% tip clearances. Note that the contour color scale in Fig. 8 was changed compared to Figs. 5 and 6, where high effectiveness is blue and low effectiveness is red. Both figures show low effectiveness at the crown (indicated in Fig. 8) and on the pressure side trailing edge, highlighted with an arrow (which is the same region that has higher Nusselt number than its adjacent pressure-side regions. Aside from the cooling hole regions, there is a higher film cooling effectiveness at about 50% *Cx* as well as at the pressure-side trailing edge corner, a region that typically observes high-heat transfer. In addition, for the last 50% C_x, the film cooling effectiveness inside the gutter is relatively high compared to the near-by pressure-side and suction-side lip overhangs.

A plot of the circumferentially-averaged film cooling effectiveness for both tip clearances, as shown in Fig 9, shows that in general, the film cooling effectiveness for the 1.0% tip gap is higher than for the 1.5% tip gap, specifically from 30—80% C_x. It is possible that the cooling films have been weakened or diluted by the increased over-tip leakage flow for the larger tip clearance. The 1.5% tip gap has higher effectiveness isolated at about 17% C_x and both tip gaps have about the same effectiveness from about 75—100% C_x. Though the 1.5% tip gap shows lower effectiveness over the crown region, the average axial-chordwise value is similar for both tip gaps due to higher effectiveness in the gutter and the recess.

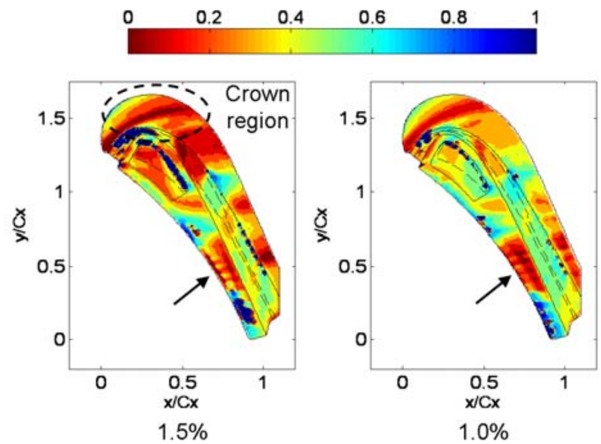

Fig. 8 Experimental film cooling effectiveness for both 1.5% and 1.0% tip gaps

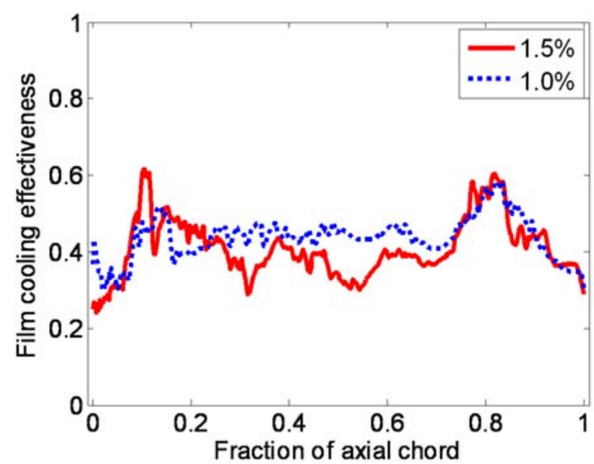

Fig. 9 Experimental circumferentially-averaged film cooling effectiveness for 1.0% and 1.5% tip clearances

The increase of Nusselt number with the addition of cooling injection warrants further discussion. Without coolant injection, it has been previously reported in [26] that the flow over the tip of the winglet is complex, transonic including shockwaves reflections. The flow structure of the OTL flow is expected to be much sensitive to the addition of the coolant injection. An enhanced turbulence mixing can be caused by the interaction between the coolant and the OTL flow. For the current transonic winglet tip study, apparently the cooling effect (net heat flux reduction) is mainly accounted by the decrease of the driving temperature over the tip surface.

Contours of the calculated local Mach number distribution, half-way between the tip surface and the casing wall, as shown in Fig. 10, can help to explain the heat transfer over the tip. At the leading edge and over the blade crown, the local Mach numbers are subsonic, which is the region that observes higher heat transfer, as previously presented in [26] for the 1.5% tip gap. Figure 10 also includes the Mach number distribution for the 1.0% tip gap, which reveals a smaller transonic region, represented by the black M=1 line, compared to the 1.5% tip gap results. Overall, the local tip Mach numbers are also less for the smaller tip gap.

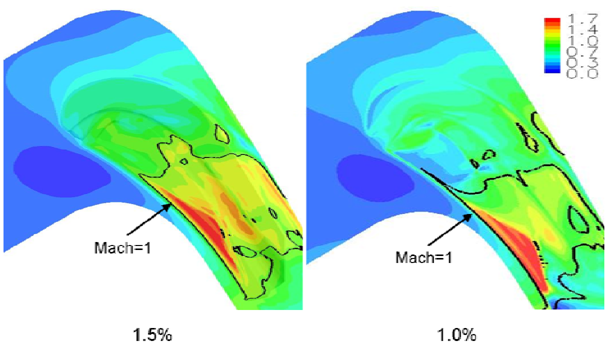

Fig. 10 Predicted Mach number for both 1.5% and 1.0% tip gaps

Mach number distributions for both tip gaps indicate that for about half of the axial chord, approximately 40—100% C_x, the tip flow is choked at the entry to the gap, with local Mach numbers exceeding 1.7. It is in this region where the variation in heat transfer and cooling effectiveness is qualitatively different compared to the subsonic region at the blade crown. This is true for both tip gaps, which is consistent with [49].

One possible reason for higher heat transfer and lower film cooling effectiveness in the region highlighted by the arrow in Fig. 8 is due to the coolant feed system inside the blade. However, another possible reason is due to the transonic nature over the tip. The transonic flow over the trailing edge region must be understood and considered when designing not only the blade, but also the cooling scheme.

6. AERODYNAMIC LOSS RESULTS

Many aerodynamic loss results relate the stagnation pressure loss normalized by the dynamic head, as was done in [56]:

$$CP_0 = \frac{P_{oi} - P_{oe}}{0.5\rho v^2} = \frac{P_{oi} - P_{oe}}{0.5\gamma P_s M^2} \tag{4}$$

However, this method calculated the loss in stagnation pressure from the inlet, which neglects the coolant pressure. As an alternative, the loss in efficiency (in the form of kinetic energy) can be used to characterize the aerodynamic loss, derived in [57]. The ideal kinetic energy can be defined in several ways [58], and the present study assumes that the mainstream and coolant expand isentropically without mixing from their supply stagnation conditions to the exit static pressure. This definition for loss coefficient, ζ, was recently used by [37] and has been modified in the present study, as shown in Eq. (5). The aerodynamic loss in the current study uses a temperature ratio of one, and therefore the temperatures and specific heats of the mainstream and coolant flow cancel.

$$\zeta = 1 - \frac{\left[\dot{m}_c + \dot{m}_m\right]\left[1 - \left(\dfrac{p_{s,local\,exit}}{p_{t,local\,exit}}\right)^{\left(\frac{\gamma-1}{\gamma}\right)}\right]}{\dot{m}_m\left[1 - \left(\dfrac{\overline{p}_{s,mid-span}}{\overline{p}_{t,inlet}}\right)^{\left(\frac{\gamma-1}{\gamma}\right)_m}\right] + \dot{m}_c\left[1 - \left(\dfrac{\overline{p}_{s,mid-span}}{\overline{p}_{t,coolant}}\right)^{\left(\frac{\gamma-1}{\gamma}\right)_c}\right]} \tag{5}$$

In Eq. (5), the numerator uses the local values of the static and total pressure. The denominator is based on the mid-span, mass-averaged exit static pressure and the average mainstream and coolant total pressures.

The experimental results for aerodynamic loss are presented for both the 1.5% and 1.0% tip gaps with and without coolant injection. Fig. 11 provides spatially-resolved loss coefficient results one axial chord downstream of the blade row for the 1.5% tip gap, where y/P represents the measurement location relative to the blade trailing edge. Results show a slight decrease in the size of the OTL loss core with coolant injection.

Figure 12 shows the loss coefficient results for the 1.0% tip gap. Compared to Fig. 11, the 1.0% tip gap shows a large decrease in the size of the loss core for the smaller tip gap, as expected. As for cooling injection for the 1.0% tip gap, the coolant slightly reduces the size of the loss core.

When considering the pitch-wise mass-averaged aerodynamic loss for both tip gaps, the coolant consistently decreases the loss coefficient from 80—95% of engine-equivalent span, as seen in Fig. 13.

Finally, the loss coefficient at a mixed-out plane is determined for both tip gaps with and without cooling using the method of [57], but for a 3-D linear cascade. The local static and total pressures in the numerator of Eq. (5) are replaced with the static and total pressure at a mixed-out plane. These results are shown in Fig. 14. The results are normalized by the loss coefficient of the uncooled winglet with 1.5% tip gap. There is a small uncertainty in the tip gap measured between the uncooled and cooled winglets due to machining tolerances as well as the uncertainty in using feeler gauges to measure the tip clearance. The effect of coolant injection on loss coefficient for the 1.0% tip gap therefore is less certain. However, despite the small uncertainty in tip clearance, it is clear that the cooled winglet has a reduced loss coefficient for the larger tip clearance, which may be indicative of an aerodynamic sealing effect created by the films, which is thought to have reduced over-tip leakage, as also observed by Krishnababu et al. [23].

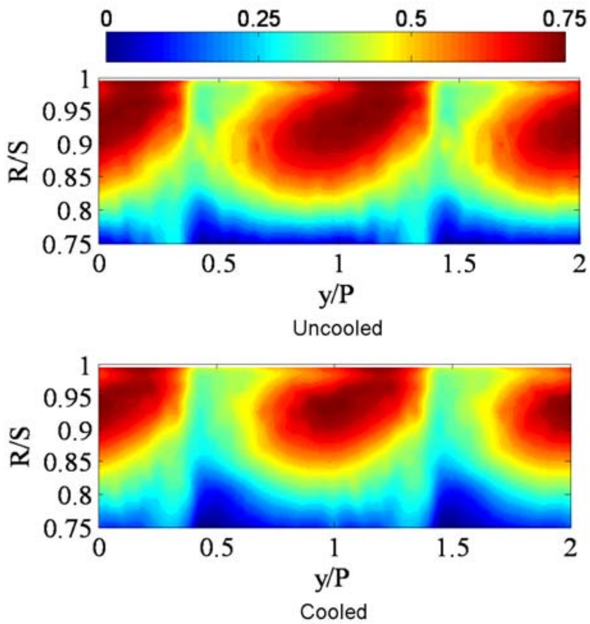

Fig. 11 Experimental loss coefficient, ζ, for 1.5%

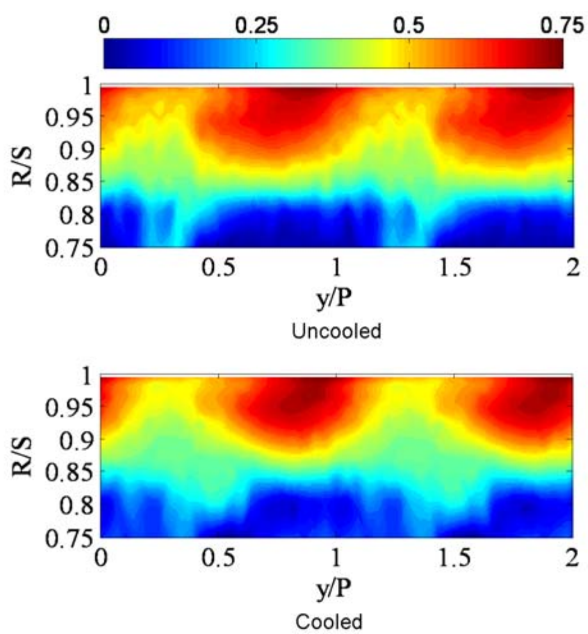

Fig. 12 Experimental loss coefficient, ζ, for 1.0%

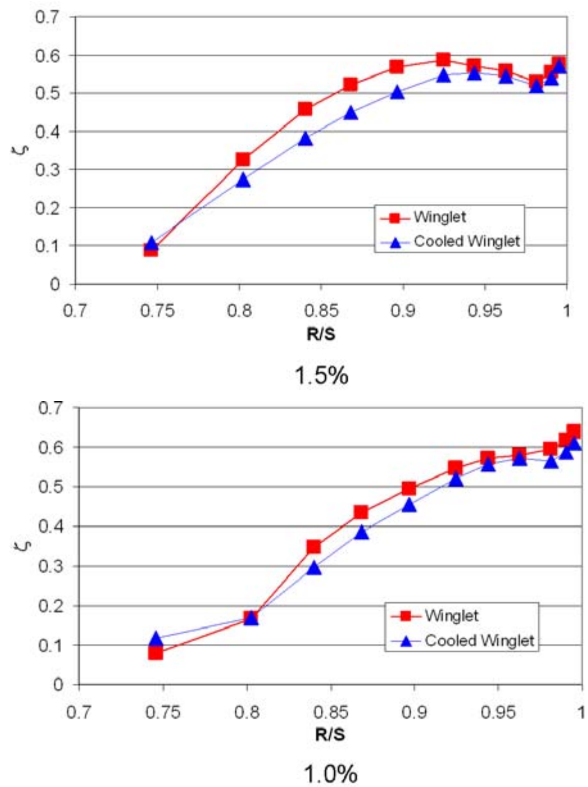

Fig. 13 Pitch-wise mass-averaged loss coefficients, ζ, for 1.5% and 1.0% tip gaps

7. NOTES ON ROTATION EFFECT

Note that the rotation effects have not been addressed in the present cascade study. Even with some previous studies which tried to address the rotation effect (such as [59,60]), to what extent a relative endwall motion at engine realistic conditions (i.e. transonic) has on the OTL flow remains an open topic. Considering the experimental difficulties, one practical method for addressing this question would be to make a greater use of the computational models to indentify how the flow changes with the introduction of rotation. In the previous study for an uncooled winglet by O'Dowd et al. [26], the effect of relative casing motion has been examined numerically after their CFD model was experimentally validated at the stationary condition. They reported that the transonic nature of the OTL flow remains the same with and without the relative casing motion, though there are noticeable changes in tip heat transfer and Mach number distribution. Further CFD studies (validations and analysis of the cooled winglet at a transonic condition) about the effect of relative motion on a cooled winglet would be useful but beyond the scope of the present paper.

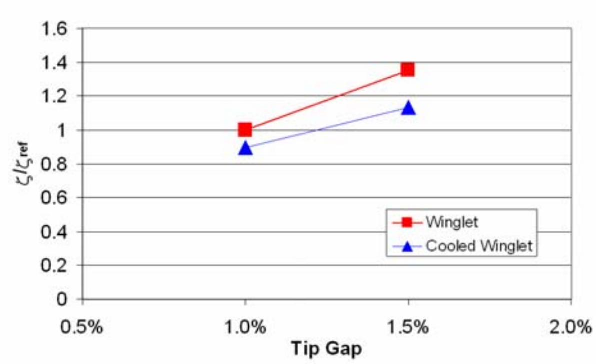

Fig. 14 Loss coefficient, ζ, for mixed-out plane

8. CONCLUSIONS

In summary, the focus of the present experimental study is on the heat transfer and aerodynamic loss of a transonic winglet tip with coolant injection for two different tip gaps. Aero-thermal results are obtained under engine-representative conditions, with exit Mach number M_{exit} of 1.0 and exit Reynolds number Re_{exit} of 1.27×10^6. Spatially-resolved heat transfer data are obtained using the transient infrared thermography using the Oxford High Speed Linear Cascade facility. Spatially-resolved blade tip aerodynamic loss coefficient (in terms of energy loss) results are presented one axial chord downstream of the blade row. These results are presented for two different tip gaps of 1.0 and 1.5 percent relative to engine-equivalent blade span.

The major conclusions are:

(1) The tip Nusselt number increases with coolant injection, consistent for both tip clearances.

(2) The tip Nusselt number increases with increased tip clearance as more mass flow passes over the tip. However, the trailing edge (90—100% C_x) shows small variation in Nusselt number.

(3) The tip film cooling effectiveness is generally higher for the 1.0% tip gap, especially from 30—80% C_x.. This may be due to cooling films that have been weakened or diluted by the increased over-tip leakage flow for the larger tip clearance.

(4) The cooled winglet aerodynamic loss coefficient results show a decrease in aerodynamic loss compared to the uncooled winglet. This is possibly due to an aerodynamic sealing effect created by the films.

(5) Aero-loss data seem to suggest that the size of the loss core associated with the over-tip leakage vortex is slightly reduced when the coolant injection is introduced. The same observation applies to both tip gaps.

NOMENCLATURE

CP_0	Pressure loss coefficient	$= (P_{oi} - P_{oe})/(0.5\gamma P_s M^2)$
Cx	Axial chord	
gap	Distance between blade tip and casing endwall	
gutter	Groove extending from leading edge to trailing edge along the camber line	
HSLC	High Speed Linear Cascade	
h	Heat-transfer coefficient [W/m^2 K]	
IR	Infrared	
k	Thermal conductivity [W/m K]	
M	Mach number	
$\dot{m}$	Mass flow rate	
Nu	Nusselt number	$= hC_x/k_{air}$
$\dot{q}$	Heat flux [W/m^2]	
OTL	Over-tip leakage	
P	Pressure or blade pitch	
PID	Proportional Band, Integral, Derivative (feedback control)	
Re	Reynolds number	
R	Span-wise (radial) distance	
R/S	Radius-wise location normalized by blade span	
RANS	Reynolds-averaged Navier-Stokes	
RMS	Root-mean-squared	
S	Blade span	
T	Temperature	
v	Velocity	
x	Axial direction	
y/P	Pitch-wise measurement location normalized by blade pitch	
y^+	Non-dimensional wall distance:	$\equiv u_t y/\nu$
ZnSe	Zinc-Selenide (IR window)	
β	Probe calibration flow (yaw) angle	
γ	Ratio of specific heat	
ζ	Aerodynamic loss coefficient	
η	Film cooling effectiveness	
ρ	Density	

Subscripts

ad	Adiabatic
c	Coolant
e, exit	exit
i	inlet
m	mainstream
rec	Recovery
s	Static
t	Total
w	Wall or surface

ACKNOWLEDGMENTS

The authors gratefully acknowledge the support of Rolls-Royce plc. for funding the experimental work and providing the test blades used in the experiments. The authors would also like to thank the skilled technicians at the University of Oxford, who ensured the test blades and instrumentation were ready for testing. The lead author is sponsored by the United States Air Force, and the views expressed in this paper do not reflect the official policy or position of the United States Air Force, Department of Defense, or the United States Government.

REFERENCES

[1] Bunker, R.S., 2001, "A Review of Turbine Blade Tip Heat Transfer in Gas Turbine Systems", Annals of the New York Academy of sciences, New York, 934, pp. 64-79

[2 Dunn, M.G., Rae, W.J., & Holt, J.L. 1984, "Measurement and Analyses of Heat Flux Data in a Turbine Stage. Part I: Description of Experimental Apparatus and Data Analysis", Journal of Engineering for Gas Turbines and Power, **106(1)**, pp. 229-233.

[3] Metzger, D.E., Dunn, M.G. & Hah, C., 1991, "Turbine Tip and Shroud Heat Transfer", ASME J. Turbomach., **113(3)**, pp. 502-507.

[4] Thorpe, S.J., Yoshino, S., Thomas, G.A., Ainsworth, R.W. & Harvey, N.W. 2005, "Blade-Tip Heat Transfer in a Transonic Turbine", Proceedings of the Institution of Mechanical Engineers, Part A: Journal of Power and Energy, **219(6)**, pp. 421-430.

[5] Bunker, R.S. Bailey, J.C., and Ameri, A.A. 2000, "Heat Transfer and Flow on the First-Stage Blade Tip of a Power Generation Gas Turbine: Part 1--Experimental Results", ASME J. Turbomach., **122(2)**, pp. 263–271

[6] Ameri, A. A., and Bunker, R. S., 2000, ''Heat Transfer and Flow on the First Stage Blade Tip of a Power Generation Gas Turbine: Part 2—Simulation Results,'' ASME J. Turbomach., **122(2)**, pp. 272–277.

[7] Azad, G. M. S., Han, J. C., Teng, S., and Boyle, R., 2000, ''Heat Transfer and Pressure Distributions on a Gas Turbine Blade Tip,'' ASME J. Turbomach., **122**, pp. 717–724.

[8] Kwak J.S. and Han, J.C., 2003, "Heat Transfer Coefficients and Film-Cooling Effectiveness on a Gas Turbine Blade Tip," ASME J. Heat Transfer, **125**, pp. 494-502.

[9] Teng, S., Han, J.C., and Azad, G.M.S. 2001, "Detailed Heat Transfer Coefficient Distributions on a Large-Scale Gas Turbine Blade Tip", Journal of Heat Transfer, **123(4)**, pp. 803-809.

[10] Newton, P.J., Krishnababu, S.K., Lock, G.D., Hodson, H.P., Dawes, W.N., Hannis, J. & Whitney, C. 2006, "Heat transfer and aerodynamics of turbine blade tips in a linear cascade", ASME J. Turbomach., **128(2)**, pp. 300-309.

[11] Bunker, R.S. and Bailey, J.C. 2000, "Effect of Squealer Cavity Depth and Oxidation on Turbine Blade Tip heat Transfer," ASME Paper 2000-GT-0155.

[12] Krishnababu, S.K., Newton, P.J., Dawes, W.N., Lock, G.D., Hodson, H.P., Hannis, J. and Whitney, C. 2007, "Aero-Thermal Investigations of Tip Leakage Flow in Axial Flow Turbines—Part I: Effect of Tip Geometry and Tip Clearance Gap", ASME J. Turbomach., **131(1)**, p. 011006 (14 pages).

[13] Kwak J.S. and Han, J.C., 2003, "Heat Transfer Coefficients on the Squealer Tip and Near Squealer Tip Regions of a Gas Turbine Blade," ASME J. Heat Transfer, **125**, pp. 669-677.

[14] Azad, G.S., Han, J. and Boyle, R.J. 2000, "Heat Transfer and Flow on the Squealer Tip of a Gas Turbine Blade", ASME J. Turbomach, **122(4)**, pp. 725-732.

[15] Nasir, H., Ekkad, S.V., Kontrovitz, D.M., Bunker, R.S. and Prakash, C. 2004, "Effect of Tip Gap and Squealer Geometry on Detailed Heat Transfer Measurements over a High Pressure Turbine Rotor Blade Tip", ASME J. Turbomach., **126(2)**, pp. 221-228.

[16] Mischo, B. Behr, T. and Abhari, R.S., 2006, "Flow physics and Profiling of Recessed Blade Tips: Impact on Performance and Heat Load," ASME Paper GT2006-91074.

[17] Dunn, M.G. and Haldeman, C.W., 2000, "Time-Averaged Heat Flux for a Recessed Tip, Lip, and Platform of a Transonic Turbine Blade," ASME J. Turbomach., **122**, pp.692-698.

[18] Ahn, J., Mhetras, S. and Han, J. C., 2005, "Film-Cooling Effectiveness on a Gas Turbine Blade Tip Using Pressure-Sensitive Paint," ASME J. Turbomach., **127(5)**, pp. 521-530.

[19] Nasir, H., Ekkad, S. V., Bunker, R. S. and Prakash, C., 2004, "Effects of Tip Gap Film Injection from Plain and Squealer Blade Tips," ASME Paper GT2004-53455.

[20] Nasir, H., Ekkad, S. V. and Bunker, R. S., 2007, "Effect of Tip and Pressure Side Coolant Injection on Heat Transfer Distributions for a Plane and Recessed Tip," ASME J. Turbomach., **129(1)**, pp. 151-163.

[21] Kwak, J. S. and Han, J. C., 2003, "Heat Transfer Coefficients and Film-Cooling Effectiveness on the Squealer Tip of a Gas Turbine Blade," J. Turbomach., **125(4)**, pp. 648-657.

[22] Newton, P. J., Lock, G. D., Krishnababu, S. K., Hodson, H. P., Dawes, W. N., Hannis, J. and Whitney, C., 2007, "Aero-Thermal Investigation of Tip Leakage Flows in Axial Flow Turbines. Part III: Tip Cooling," ASME Paper GT2007-27368.

[23] Krishnababu, S. K., Hodson, H. P., Booth, G. D., Lock, G. D. and Dawes, W. N., 2008, "Aero-Thermal Investigation of Tip Leakage Flow in a Film Cooled Industrial Turbine Rotor," ASME Paper GT2008-50222.

[24] Papa, M., Goldstein, R. J. and Gori, F., 2003, "Effects of Tip Geometry and Tip Clearance on the Mass/Heat Transfer from a Large-Scale Gas Turbine Blade," ASME J. Turbomach., **125(1)**, pp. 90-96.

[25] Saha, A.K., Acharya, S., Prakash, C., Bunker, R.S., 2003, "Blade Tip Leakage Flow and Heat Transfer with Pressure Side Winglet", ASME Paper GT2003-38620.

[26] O'Dowd, D. O., Zhang, Q., He, L., Oldfield, M. L. G., Ligrani, P. M., Cheong, B. C. Y. and Tibbott, I., 2010, "Aero-Thermal Performance of a Winglet at Engine Representative Mach and Reynolds Numbers," ASME Paper GT2010-22794, to be published in ASME J. Turbomach.

[27] Denton, J.D., 1993, "Loss Mechanisms in Turbomachines," ASME J. Turbomach., **115**, pp. 621–656.

[28] Xiao, X., McCarter, A.A. and Lakshminarayana, B., 2001, "Tip Clearance Effects in a Turbine Rotor: Part I—Pressure Field and Loss," ASME J. Turbomach., **123**, pp. 296-304.

[29] McCarter, A.A., Xiao, X. and Lakshminarayana, B., 2001, "Tip Clearance Effects in a Turbine Rotor: Part II— Velocity Field and Flow Physics," ASME J. Turbomach., **123**, pp. 305-313.

[30] Rao, N.M,, Gumusel, B. Kavurmacioglu, L. and Camci, C., 2006, "Influence of Casing Roughness on the Aerodynamic Structure of Tip Vortices in an Axial Flow Trubine," ASME Paper GT2006-91011.

[31] Main, A.J., Day, C.R.B., Lock, G.D. and Oldfield, M.L.G., 1996, "Calibration of a Four-Hole Pyramid Probe and Area Traverse Measurements in a Short-Duration Transonic Turbine Cascade Tunnel," Experiments in Fluids, **21**, pp. 302-311.

[32] Bindon, J.P. 1989, "Measurement and Formation of Tip Clearance Loss", ASME J. Turbomach., **111**, pp. 257-263.

[33] Yamamoto, A., 1989, “Endwall Flow/Loss Mechanisms in a Linear Turbine Cascade with Blade Tip-Clearance,” ASME J. Turbomach,**111**, pp. 264-275.
[34] Palafox, P., Oldfield, M.L.G., LaGraff, J.E. and Jones, T.V., 2008, “PIV Maps of Tip Leakage and Secondary Flow Fields on a Low Speed Turbine Blade Cascade with Moving Endwall,” ASME J. Turbomach., **130(1)**, pp. 011001.
[35] Heyes, F. J. G., Hodson, H. P. and Dailey, G. M., 1992, “The Effect of Blade Tip Geometry on the Tip Leakage Flow in Axial Turbine Cascades,” ASME J. Turbomach., **114(3)**, pp. 643–651.
[36] Key, N.L, and Arts, T. 2006, “Comparison of Turbine Tip Leakage Flow for Flat Tip and Squealer Tip Geometries at High-speed Conditions”, ASME J. of Turbomach, **128**, pp. 213-220.
[37] Hofer, T. and Arts, T. 2009, “Aerodynamic Investigation of the Tip Leakage Flow for Blades with Different Tip Squealer Geometries at Transonic Conditions,” ASME Paper GT2009-59909.
[38] Wadia, A. R. and Booth, T. C., 1982, “Rotor-Tip Leakage: Part II—Design Optimization through Viscous Analysis and Experiment," Journal of Engineering for Power, **104(1)**, pp. 162-169.
[39] Yaras, M.I., Sjolander, S.A. & Kind, R.J. 1992, “Effects of Simulated Rotation on Tip Leakage in a Planar Cascade of Turbine Blades: Part II - Downstream Flow Field and Blade Loading”, ASME J. Turbomach., **114**, pp. 660-667.
[40] Dey, D. and Camci, C., 2001, “Aerodynamic Tip Desensitization of an Axial Turbine Rotor Using Tip Platform Extensions”, ASME Paper 2001-GT-0484.
[41] Schabowski, Z. and Hodson, H.P., 2007, “The Reduction of Over Tip Leakage Loss in Unshrouded Axial Turbines Using Winglets and Squealers,” ASME Paper GT2007-27623.
[42] Schabowski, Z., Hodson, H., Giacche, D., Power, B. and Stokes, M. R., 2010, “Aeromechanical Optimisation of a Winglet-Squealer Tip for an Axial Turbine,” ASME Paper GT2010-23542.
[43] Harvey, N.W. and Ramsden, K., 2001, “A Computational Study of a Novel Turbine Rotor Partial Shroud,” ASME J. Turbomach., **123**, pp. 534-543.
[44] Harvey, N.W., Newman, D.A., Haselbach, F., and Willer L., 2006, “An Investigation Into a Novel Turbine Rotor Winglet. Part 1: Design and Model Rig Test Results,” ASME Paper GT2006-90456.
[45] Willer, L., Newman, D.A., Haselbach, F., and Harvey, N.W., 2006, “An Investigation Into a Novel Turbine Rotor Winglet. Part 2: Numerical Simulation and Experimental Results,” ASME Paper GT2006-90459.
[46] Moore, J., Moore, J. G., Henry, G. S. and Chaudhry, U., 1989, “Flow and Heat Transfer in Turbine Tip Gaps," ASME J. Turbomach., **111(3)**, pp. 301-309.
[47] Zhang, Q., ODowd, D. O., He, L., Wheeler, A. P. S., Ligrani, P. M. and Cheong, B. C. Y., 2011, ”Over-Tip Shock Wave Structure and its Impact on Turbine Blade Tip Heat Transfer,” ASME J. Turbomach., to be published. Much of this was presented at the International Symposium on Heat Transfer in Gas Turbine Systems, International Centre for Heat and Mass Transfer.
[48] Wheeler, P.S., Atkins, N.R. and He, L., 2009, “Turbine Blade Tip Heat Transfer in Low Speed and High Speed Flows”, ASME Paper GT2009-59404.
[49] Zhang, Q., O'Dowd, D. O., He, L., Oldfield, M. L. G. and Ligrani, P. M., 2010, “Transonic Turbine Blade Tip Aero-Thermal Performance with Different Tip Gaps: Part I—Tip Heat Transfer,” ASME Paper GT2010-22779, to be published in ASME J. Turbomach.
[50] Gillespie, D.R.H, Wang, Z. & Ireland, P.T. 1995, “Heating Element”, British Patent Application PCT/GB96/2017
[51] O’Dowd, D.O., Zhang, Q., He, L., Ligrani, P.M. and Friedrichs, S., 2011, “Comparison of Heat Transfer Measurement Techniques on a Transonic Turbine Blade Tip,” ASME J. Turbomach., **133(2)**, pp. 021028 (10 pages)
[52] Oldfield, M.L.G. 2008, “Impulse Response Processing of Transient Heat Transfer Gauge Signals”, ASME J. Turbomach., **130(2)**, pp. 021023 (9 pages).
[53] Kline, S.J. and McClintock, F.A. 1953, “Describing Uncertainties in Single-Sample Experiments”, Mechanical Engineering, **75**(January), pp. 3-8.
[54] Moffat, R.J. 1988, “Describing the Uncertainties in Experimental Results”, Experimental Thermal and Fluid Science, **1**, pp. 3-17.
[55] Coleman H.W., and Steele, W.G., 1989, Experimentation and Uncertainty Analysis for Engineers, John Wiley & Sons, New York, USA.
[56] O’Dowd, D.O., Zhang, Q., Usandizaga, I., He, L., and Ligrani, P.M., 2010, “Transonic Turbine Blade Tip Aero-Thermal Performance with Different Tip Gaps: Part II—Tip Aerodynamic Loss,” ASME Paper GT2010-22780
[57] Main, A.J., Oldfield, M.L.G., Lock G.D. and Jones, T.V., 1997, “Free Vortex Theory for Efficiency Calculations from Annular Cascade Data,” ASME J. Turbomach., **119(3)**, pp. 257-263.
[58] Young, J.B. and Horlock, J.H, 2006, “Defining the Efficiency of a Cooled Turbine”, ASME J. Turbomach., **128(4)**, pp. 658-667.
[59] Krishnababu, S.K., Dawes, W.N., Hodson, H.P., Lock, G.D., Hannis, J. and Whitney, C. 2007, “Aero-Thermal Investigations of Tip Leakage Flow in Axial Flow Turbines—Part II: Effect of Tip Geometry and Tip Clearance Gap”, ASME J. Turbomach., **131(1)**, p. 011007 (10 pages).
[60] Srinivasan, V., and Goldstein, R. J., 2003, “Effect of Endwall Motion on Blade Tip Heat Transfer”, ASME J. Turbomach., **125(2)**, pp. 267-273.

